Electronic Journal of Structural Engineering

Original Article

Cite this: DOI:10.56748/ejse.25656

Received Date: 06 July 2024
Accepted Date: 08 January 2025

1443-9255
https://ejsei.com/ejse

Dynamic Response Analysis of Dowel-Slot Grouting Assembly Station Under Earthquake Action

Guanhua Cui [a], Tao Yang [a, b], Kunjie Tang [a], Jiawei Xu [a], Yuwei Zhang [a,b], Junling Qiu [a*]

[a] School of Highway, Chang'an University, Xi'an 710064, China
[b] Sichuan Dujinshan rail transit Ltd, Chengdu, Sichuan 610000, China
*Corresponding author: junlingqiu@chd.edu.cn

Abstract

In order to study the seismic performance of Dowel-Slot Grouting Assembly Station, the displacement and stress changes of the station and the cast-in-place station under horizontal, vertical and horizontal-vertical coupled earthquakes were compared by the finite element numerical simulation method based on a subway station in Changchun. The results indicate that the two stations have the same stress concentration position and the same weak point under different seismic actions, and both meet the aseismic requirements. Compared with the traditional cast-in-place station, the assembly station has obvious advantages in vertical seismic performance, but the horizontal seismic ability is relatively weak, and the difference of the displacement Angle between layers is 20%~60%. Compared with the difference of 46.43% in the maximum seismic stress and 28.51% in the vertical seismic time, the difference of 58.02% in the coupled seismic action shows that the stress concentration is more obvious. It provides reference for further optimization of assembly station.

Keywords

Seismic load, Assembly station, Dynamic response, Numerical simulation

Introduction

With the continuous development of urban construction in China, the utilization rate of urban underground space has been increasing year by year. The proportion of newly added urban underground construction area to the completed above ground construction area has risen from 15% in 2015 to 22% in 2020. China's "The 14th Five-Year Plan" explicitly emphasizes accelerating the construction of urban rail transit and promoting the modernization of urban transportation. Meanwhile, the State Council of China has proposed to focus on the "green and low-carbon" concept, accelerate the construction of green transportation infrastructure, and adopt environmentally friendly, energy-efficient, and low-carbon technologies to reduce energy dependence and carbon emissions. In this context, assembly stations, which have advantages such as reduced pollution and shorter construction periods compared to traditional cast-in-place structures, are favored (Yang, 2021). Assembly stations use advanced mortise and groove grouting technology to manufacture and pre-assemble components in advance and assemble them on-site. With guaranteed quality, this structure demonstrates significant advantages in improving construction efficiency and shortening project duration.

Compared to traditional cast-in-place structures, the existence of prefabricated joints leads to a decrease in the overall integrity of the underground structure, affecting load-bearing characteristics, seismic response, and overall stability and safety (Yang, 2018). The commonly used segment assembly method for shield tunnels is limited to circular segments and cannot be directly applied to irregular subway station structures. Song et al. (2021) conducted numerical simulations using ABAQUS software on a double-span column-free assembly subway station, studying the characteristics of internal force distribution, providing a basis for the design of this type of subway station. Du et al. (2017) through numerical simulation and low-cycle fatigue tests, studied the seismic performance of an assembly integral station structure in Beijing. The results showed that the prefabricated assembly structure's nodes performed well compared to the cast-in-place structure, with a significant reduction in energy consumption. While the above studies used numerical simulations and experimental analyses to examine the structural performance of different prefabricated subway stations, the engineering perspective is not comprehensive enough. Further in-depth research is needed to better leverage the advantages of Assembly structures.

Based on the Changchun subway station project, this paper analyzes the contact behavior of assembly joints, addresses the practical application issues of dynamic constitutive behavior, and utilizes ABAQUS software to model and analyze the changes in displacement and stress at key points of two different station structures under horizontal, vertical, and coupled horizontal-vertical seismic loads. The aim is to reveal the response of assembly stations under seismic dynamics and provide a scientific basis for further improving the seismic performance of subway stations.

1. Project profile

Due to issues such as the solidification temperature, humidity, and curing time, the traditional cast-in-place concrete construction method is not suitable for use in the cold and prolonged winter of the Northeast high-latitude regions. The construction method of prefabricating components in the factory and assembling them on-site, using advanced dovetail grouting technology, is highly favored due to its fast construction speed, reduction in waste and wood consumption, high level of mechanization, and simple installation. The surrounding environment and location are illustrated in Figure 1.

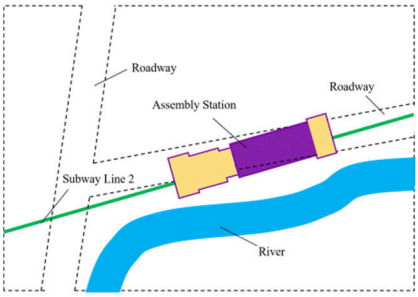

Fig. 1 Surroundings and location

1.1 Geological conditions

According to on-site geological survey data and relevant research materials, the surface soil of the Changchun Line 2 single-arch large-span mortise and groove grouting assembly station is mainly composed of artificial miscellaneous fill. Beneath it are sequential layers of silty clay 1, silty clay 2, and weathered mudstone. Table 1 provides information on the thickness, material parameters, and mechanical parameters of the geological formations.

The site has two layers of groundwater: the first layer is confined aquifer, with a depth ranging from 2.60 to 4.70 meters and an elevation between 213.00 and 234.96 meters. The second layer is mudstone fissure water, existing within the fissures of the mudstone. It mainly receives recharge from the upper confined aquifer and lateral runoff and is discharged through runoff and artificial extraction. No sand layer or shallow confined aquifer has been identified. This study does not consider the effects of groundwater issues such as soil-water flow coupling and soil liquefaction.

Table 1. Basic parameters of rock and soil mass

Rock and soil mass designation	Thickness (m)	Elastic modulus (kPa)	Poisson's ratio	Densit (kg/m³)	Frictional angle (°)	Cohesive force (kPa)
Artificial miscellaneous fill	4	7×104	0.37	1.9×10³	16.3	10
silty clay1	6	1.3×105	0.32	1.95×10³	25.94	40
silty clay2	14	2×105	0.27	1.98×10³	29.53	50
Weathered mudstone	undrilled	5×105	0.25	1.99×10³	31.26	74.3

1.2 Station structure and detailed dimensions

The assembly station is a single-arch large-span structure with a height of 17.45 meters, an upper width of 21.3 meters, and a lower width of 20.5 meters. The structure is divided into two layers with a cast-in-place (or assembled) layer in the middle, and there are cast-in-place columns on the first layer, as shown in Figure 2. The assembly station is assembled from as many as 88 assembly rings, each consisting of 7 assembly blocks. The joints between rings, except for the 4L blocks (4R blocks), are staggered, while the rest are butt jointed. The physical and mechanical parameters of various components of the station structure are provided in Table 2 (Ding et al., 2018, 2019).

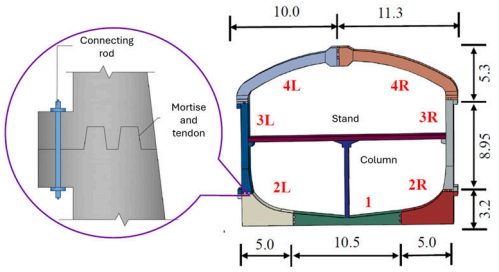

Fig. 2 Schematic diagram of assembly station structure and detailed structure (unit: m)

Table 2. Station component parameters

Component name	Compressive strength of concrete (MPa)	Elastic modulus (kPa)	Poisson's ratio	Density (kg/m³)
Four Assembly parts	50	3.45×10⁷	0.2	2.4×10³
Cast-in-place laminate	40	3.25×10⁷	0.2	2.4×10³
Cast-in-place column	50	3.45×10⁷	0.2	2.4×10³

2. Construction of dynamic finite element model

2.1 Model overview

To reduce computational costs, a paired structure consisting of a front ring and a rear ring is chosen as the basic research object, resulting in 44 identical groups for the assembly station, as illustrated in Figure 3. The connections between 2L, 2R blocks, layer plates, and 1 block with the columns are made using a "tie" approach. The computational model has a width of 150 meters in the x-direction (lateral), which is seven times the effective width of the station structure. In the y-direction (longitudinal), the width is 4 meters, corresponding to the width of a 2-ring station structure. In the z-direction (vertical), the distance from the ground surface is 3.5 meters (buried depth of 3.5 meters). The distance between the lower part of the station structure and the model's lower surface is three times the effective width of the model, resulting in a vertical dimension of 75 meters. The construction of the three-dimensional dynamic numerical model for the assembly station is based on an equivalent linear viscoelastic constitutive model (Tao et al., 2019).

In order to accurately reflect the mechanical characteristics of rock mass and station structure in the model, the three-dimensional mesh is divided based on the C3D8 unit provided in ABAQUS. According to the study of wave mechanic and the related wave parameters of soil mass in Table 3, the grid of the assembly ring is specified as 0.2m. At the same time, in order to obtain more accurate mesh division results and fit the size of the assembly, the size of the surrounding rock mass is divided into 0.5m~2m. The whole model of mesh division is completed, as shown in Figure 3.

Simultaneously, in order to better assess the seismic performance of the assembly station, this study, based on the characteristics of one-time forming in the cast-in-place method, employs a similar modeling approach to establish a comparison model for a cast-in-place station with the same structural dimensions and materials, as shown in Figure 3.

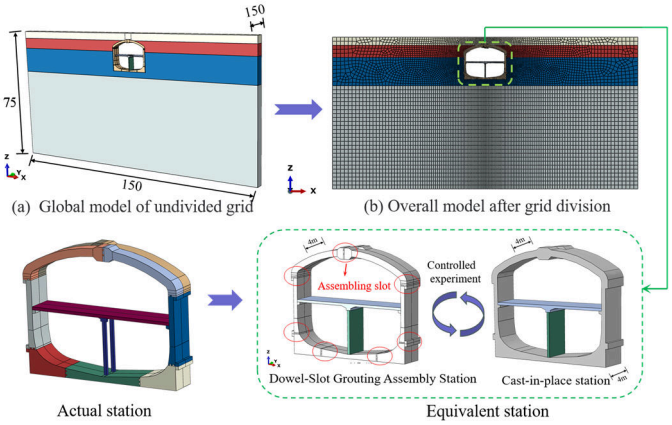

Fig. 3 Establishment of soil and station model (unit: m)

Table 3. Basic parameters of rock and soil mass

Soil layer numbering	Name	Shear wave velocity c_s (m/s)	Longitudinal wave velocity c_p (m/s)	Soil lateral coefficient $(1-\sin\varphi)$
1	Artificial Fill	115.9	191.9	0.72
2	Silty Clay 1	158.9	258.2	0.56
3	Silty Clay 2	199.4	317.8	0.51
4	Weathered Mudstone	317	501.2	0.48

2.2 Seismic wave processing and input

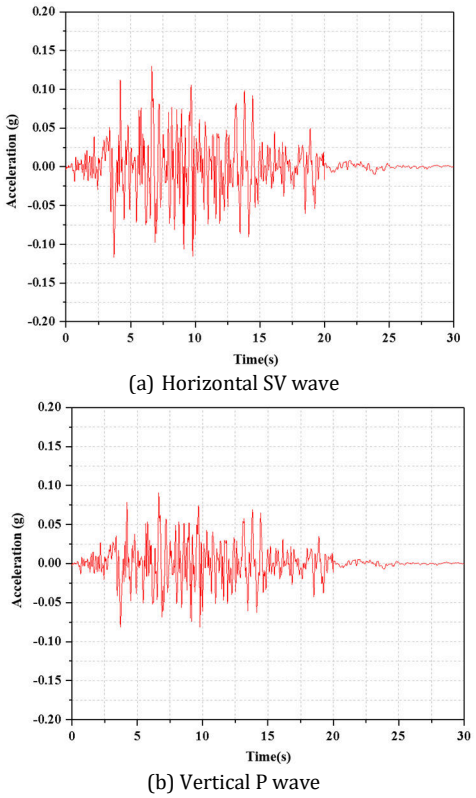

Fig. 4 Seismic wave acceleration time history (a-t) curve

The seismic safety assessment document for the assembly station uses an artificial seismic wave as the input seismic wave for this model. The seismic wave is input using the method of directly constraining free degrees of freedom with input dynamic time history. The duration of the

horizontal motion is 30 seconds, and the acceleration is 0.13g, as shown in Figure 4(a). According to the specification (Ding et al., 2019), the vertical seismic acceleration peak is taken as 70% of the horizontal direction, i.e., 0.091g, as shown in Figure 4(b).

3. Two stations displacements under different earthquake

3.1 Side wall deformation

During the entire seismic process, the horizontal relative deformation (U1) of the left and right walls of the assembly station and the cast-in-place station are shown in Figures 5 to 7. Comparative analysis reveals that under horizontal seismic action, the deformation of both stations is composed of elastic and plastic components, and the curves maintain the same shape throughout. However, due to multiple joints in the assembly station, there is discontinuity in the stiffness of the side wall structure, leading to a reduction in the horizontal seismic performance capacity of the structure, with relatively larger deformations.

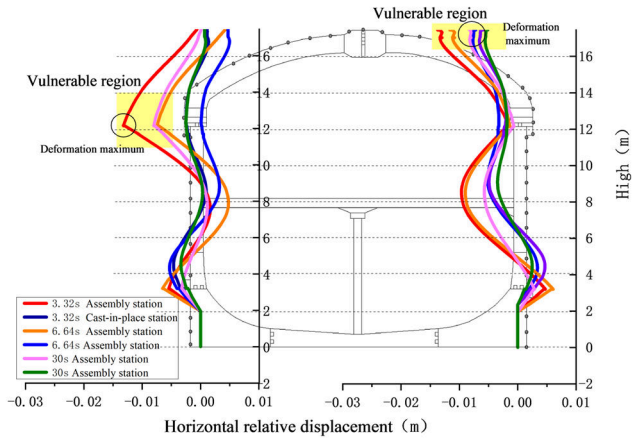

Fig. 5 Lateral wall deformation of two stations under horizontal ground motion input

During the vertical seismic action, the deformation of the left and right walls of both stations exhibits highly coordinated symmetry, indicating that the staggered structure at the top of the assembly station has a relatively small horizontal force impact under vertical seismic wave.

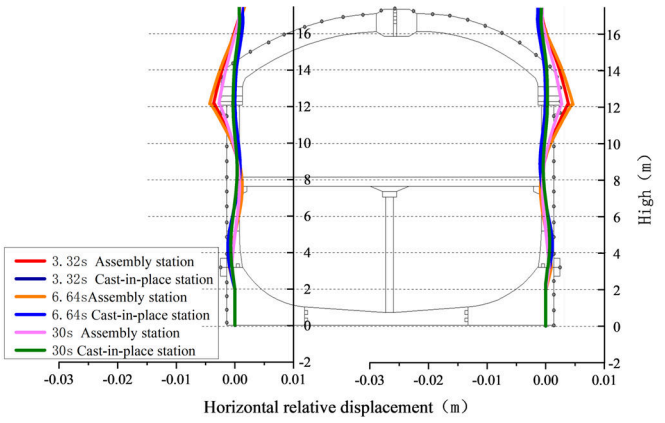

Fig. 6 Lateral wall deformation of two stations under vertical ground motion input

Under horizontal-vertical coupled seismic wave, both stations' side walls exhibit a certain degree of overall displacement, with the assembly station experiencing a larger degree of displacement. Additionally, the side walls of both stations undergo severe local deformations, but there are significant differences in the deformation curves between the two stations. The curve deformation discontinuity resulting from the stiffness discontinuity in the assembly station is most pronounced in horizontal seismic wave and bidirectional coupled seismic wave, while this discontinuity tends to diminish in vertical seismic wave.

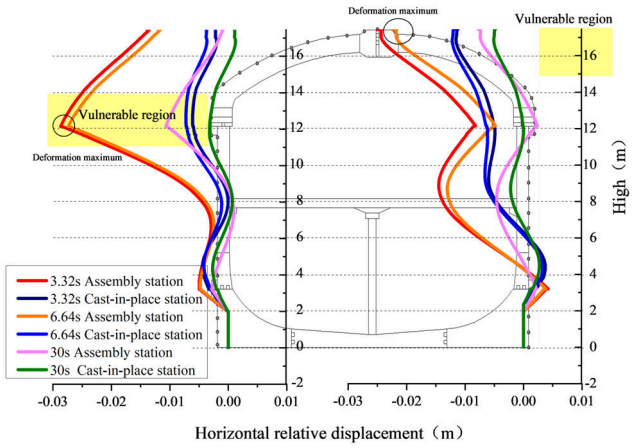

Fig. 7 Lateral wall deformation of two stations under horizontally vertical coupling ground motion input

3.2 Inter-story drift angles

Table 3 presents the inter-story drift angles of the left and right walls of both stations under different seismic inputs. The inter-story drift angles of both station structures are below the limit of 1/250, satisfying the seismic requirements for the stations. Based on calculations for the assembly station, the relative differences in inter-story drift angles between the two stations were determined. Under horizontal seismic input, the relative differences in inter-story drift angles between the upper and lower levels of the two stations range from 20% to 60%, indicating that the presence of the dovetail grouting assembly structure significantly reduces the seismic performance of the traditional cast-in-place station. In the cast-in-place station, the inter-story drift angles of the upper level are consistently smaller than those of the lower level, demonstrating greater stability in the upper structure. However, the relative magnitudes of inter-story drift angles between the upper and lower levels of the assembly station vary, indicating that the assembly structure not only reduces seismic performance but also affects vulnerable points in the station structure.

Vertical seismic threats to the horizontal direction of the station structure are minimal. Comparing the relative differences in inter-story drift angles between the upper and lower levels of the assembly and cast-in-place stations under horizontal seismic wave, it is evident that the horizontal trends of both stations during horizontal seismic wave are similarly applicable under vertical seismic wave. However, the relative differences in inter-story drift angles for the upper levels of both stations are greater, while those for the lower levels are smaller.

Under horizontal-vertical coupled seismic wave, the inter-story drift angles of the upper and lower levels in the assembly station are larger than those in the cast-in-place station, indicating that the presence of the mortise and groove grouting region reduces the seismic capacity of the underground station. The inter-story drift angles of the upper level in the assembly station exhibit the fastest decline in seismic performance, reaching relative differences of over 50% compared to the upper-level inter-story drift angles in the cast-in-place station, indicating that the upper structure of the assembly station is significantly affected by seismic waves and is a relatively vulnerable area.

Table 3. The displacement Angle between the left and right walls of the two stations

Seismic wave	Floor	Left side wall $[\theta_p]$			Right side wall $[\theta_p]$		
		Assembly station	Cast-in-place station	Relative difference	Assembly station	Cast-in-place station	Relative difference
Horizontal direction	substratum	1/756	1/1026	26.32%	1/568	1/925	38.59%
	superstratum	1/745	1/1831	59.31%	1/862	1/1926	55.24%
Vertical direction	substratum	1/3875	1/4185	7.41%	1/4629	1/4149	11.57%
	superstratum	1/1500	1/6506	76.94%	1/1592	1/6605	75.89%
Horizontal and vertical coupling	substratum	1/649	1/819	20.76%	1/461	1/926	50.22%
	superstratum	1/390	1/581	32.87%	1/483	1/1333	63.77%

In the cast-in-place station under both unidirectional and bidirectional coupled seismic actions, the inter-story drift angles of the upper level are consistently smaller than those of the lower level, demonstrating that the lower level of the cast-in-place station is a relatively weak area. However, the relative magnitudes of inter-story drift angles between the upper and lower levels of the assembly structure are dynamically changing, indicating that the relationship between unidirectional and bidirectional seismic actions is not a simple superposition, and there are still unclear interactions between the two types of unidirectional seismic actions that constitute bidirectional coupled seismic wave.

4. Mechanical property analysis of station structure

4.1 Horizontal seismic action

Under horizontal seismic wave, the locations experiencing compression and tension in both the assembly station and the cast-in-place station are distributed similarly, concentrating at the joints 2L-3L (2R-3R) and 3L-4L (3R-4R) in the assembly station structure. Additionally, both are at their most unfavorable state at the moment of peak acceleration (6.64 seconds), as shown in Figure 8(a) and (b). However, the compressed area in the assembly station is relatively smaller, with the maximum seismic stress (5.14 MPa) being 46.43% higher than that in the cast-in-place station (3.51 MPa). This indicates that the assembly station intensifies stress concentration, amplifying the tendency for rotation from tension to compression zones at the joints. This leads to changes in the seismic performance of the structure in both horizontal and vertical directions, resulting in a decrease in horizontal resistance and an increase in vertical resistance.

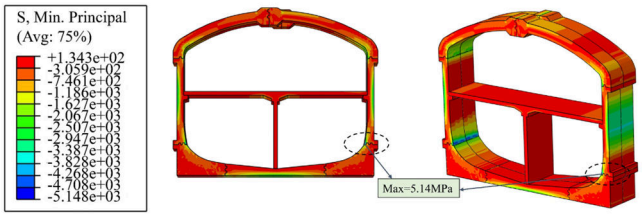

(a) mortise and slot grouting assembly type station

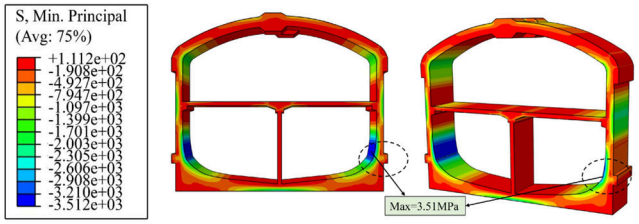

(b) cast-in-place station

Fig. 8 Seismic stress state of two stations under horizontal earthquake

4.2 Vertical seismic excitation

Under vertical seismic wave, the stress distribution in the structures of both stations is essentially the same, and the maximum deformation still occurs at the moment of peak acceleration (6.64 seconds). The maximum seismic stress in the assembly station (3.11 MPa) is 28.51% higher than that in the cast-in-place station (2.43 MPa), as shown in Figure 9(a) and (b). Compared to horizontal seismic waves, the seismic stresses in both stations are smaller and exhibit less variation under vertical seismic waves. Simultaneously, there is a more pronounced stress concentration at the back of joint 2L(R) and the contact area with the layer plate in the assembly station structure. This phenomenon is more evident under vertical seismic waves than under horizontal seismic waves.

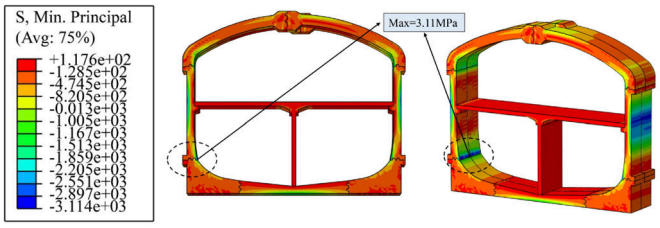

(a) mortise and slot grouting assembly type station

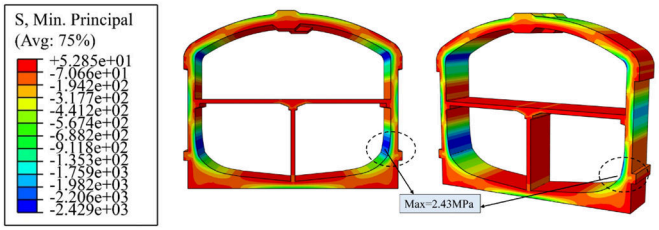

(b) cast-in-place station

Fig. 9 Seismic stress state of two stations under vertical earthquake

4.3 Coupled horizontal-vertical seismic action

Under the coupled seismic wave action, the maximum seismic stress in the assembly structure is 7.38 MPa, which is a 58.02% increase compared to the cast-in-place station (4.67 MPa). The seismic stress distribution in the structures of both stations is shown in Figure 10(a) and (b). Similar to the seismic stress distribution under horizontal and vertical seismic wave, under coupled seismic wave action, the maximum compressive stress in both station structures occurs at the joints 2L-3L (2R-3R) and 3L-4L (3R-4R) of the assembly station. However, there is no pronounced stress concentration at the back of joint 2L(R) and the contact area with the layer plate under the coupled seismic wave action, as observed under vertical seismic wave.

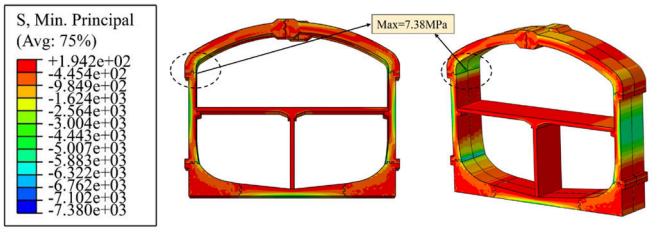

(a) mortise and slot grouting assembly type station

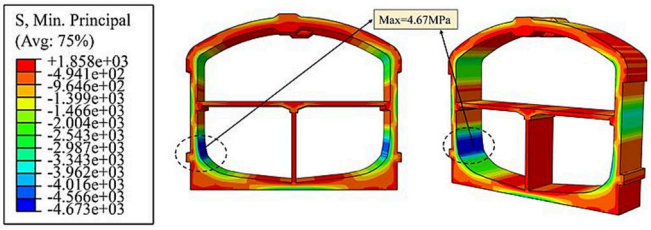

(b) cast-in-place station

Fig. 10 Seismic stress state of two stations under horizontally vertical coupling earthquake

Analyzing the seismic stress in the structures of both stations under the different seismic waves as shown in Table 4, it is evident that under the coupled seismic wave action, the vulnerable points (stress concentration points) in both station structures are consistent with those under unidirectional seismic wave action, but the maximum seismic stress is higher than that under horizontal or vertical seismic wave. This indicates that the input direction of the seismic wave does not alter the vulnerable points in the structure, but there is a certain amplification effect when unidirectional waves are superimposed. The difference in maximum seismic stress between the two station structures reaches 58.02% under coupled seismic wave action, which is higher than the differences under horizontal seismic wave (46.43%) or vertical seismic wave (28.51%). This suggests that the magnitude of peak acceleration is directly related to the stress and displacement in the station structure.

Table 4. The maximum seismic stress of two station structures under the action of seismic waves in different directions

Seismic wave	Cast-in-place station (MPa)	Assembly station (MPa)	Difference value (MPa)	Offset ratio (MPa)
Horizontal direction	3.51	5.14	1.63	46.43%
Vertical direction	2.42	3.11	0.69	28.51%
Horizontally vertical coupling	4.67	7.38	2.71	58.02%

5. Conclusion

(1) Both stations primarily exhibit elastic deformation, supplemented by residual deformation. Whether under horizontal, vertical, or coupled seismic wave, the inter-story displacement angles are all below the limit of 1/250, meeting seismic requirements. Additionally, the stress concentration locations and structural vulnerable points remain the same for both stations under different seismic actions.

(2) Compared to the traditional method of overall cast-in-place construction, the assembly station demonstrates superior vertical seismic performance. However, under horizontal seismic wave, the relative difference in inter-story displacement angles for the assembly station compared to the cast-in-place station ranges from 20% to 60%, indicating weaker seismic performance. Specifically, the upper structure of the assembly station is more sensitive to seismic waves, with the relative difference in inter-story displacement angles exceeding 50% under both unidirectional and bidirectional coupled seismic wave, placing it in a relatively vulnerable zone.

(3) Under coupled seismic wave action, both the cast-in-place station and the assembly station experience an increase in maximum seismic stress, indicating a certain level of amplification when unidirectional waves are superimposed. The assembly station, due to factors such as stiffness discontinuity and the opening of assembly station, exhibits significant stress concentration. As a result, under horizontal, vertical, and coupled seismic wave, the maximum seismic stress for the two stations differs by 46.43%, 28.51%, and 58.02%, respectively.

Acknowledgments

This work was jointly supported by the National Natural Science Foundation of China (No. 52278393, 52208386, 52078421), the Key R&D Program of Shaanxi Province (2024SF-YBXM-635, 2023-YBSF-511), the Fundamental Research Funds for the Central Universities, CHD (300102213202), and the Natural Science Basic Research Program of Shaanxi Province. We also acknowledge the editor for the valuable suggestion.

Declaration of Competing Interest

The authors declare that they have no known competing financial interests or personal relationships that could have appeared to influence the work reported in this paper.

Data availability

Data will be made available on request.

Reference

Ding, P. & Tao, L. J. & Yang, X. R. et al. (2019) Force transfer and Deformation mechanism of Prefabricated single-loop structure in station. Journal of Southwest Jiao tong University: 55(05): 1-10. (in Chinese)

Ding, P. & Tao, L. J. & Yang, X. R. et al. (2019). Three-Dimensional Dynamic Response Analysis of a Single-Ring Structure in a Prefabricated Station. Sustainable Cities and Society, 45: 271-286. https://doi.org/10.1016/j.scs.2018.11.010

Ding, P. & Yang, X. R. & Gao, X. Y. et al. (2018). Horizontal and vertical seismic responses of single-arch long-span prefabricated station. Journal of Heilongjiang University of Science and Technology, 28(06): 630-637. (in Chinese)

Du, X. L. & Liu, H. T. & Lu, C. et al. (2017). Research on seismic performance of side Wall bottom joints of Assembled integrated stations. Journal of Civil Engineering, 50(04):38-47. https://doi.org/10.15951/j.tmgcxb.2017.04.005. (in Chinese)

Song, R.& Zhang J. Q.& Cui T., et al. (2021). Analysis of Structural Mechanical characteristics of double-span pillar-less assembled stations. Standard Railway Design. 65(2): 123-127, 178. https://doi.org/10.13238/j.issn.1004-2954.202005170005. (in Chinese)

Tao, L. J. & Ding, P. & Shi, C. et al. (2019) Shaking Table Test on Seismic Response Characteristics of Prefabricated Station Structure. Tunnelling and Underground Space Technology, 91. https://doi.org/10.1016/j.tust.2019.102994

Tao, L. Jin. & Li, Z. Y. & Yang, X. R. et al. (2018) Research on Mechanical Behavior of prefabricated station Structures after Assembling rings based on ABAQUS. Modern Tunnel Technology. 55(05): 115-123. https://doi.org/10.13807/j.cnki.mtt.2018.05.014

Yang, X. R. (2018). Research strategy on new technology of precast assembly in station [J]. Urban Rapid Transit. 31(01):78-85. (in Chinese)

Yang, X. R. (2021). Development Status of and Outlook for Construction Technology for Prefabricated Metro Stations in China. Tunnel Construction (Chinese and English), 41(11):1849-1870. https://link.cnki.net/urlid/44.1745.U.20211130.1653.018. (in Chinese)

Disclaimer